

REVIEW OF W AND Z PRODUCTION AT THE TEVATRON

Cecilia E. GERBER

Fermi National Accelerator Laboratory
P.O. Box 500, Batavia, IL 60510, USA
(for the DØ and CDF Collaborations)

Presented at XXXIIIrd Recontres de Moriond
QCD AND HIGH ENERGY HADRONIC INTERACTIONS
Les Arcs, Savoie, France
March 21–28, 1998

The CDF and DØ collaborations have used recent data taken at the Tevatron to perform QCD tests with W and Z bosons decaying leptonically. DØ measures the production cross section times branching ratio for W and Z bosons. This also gives an indirect measurement of the total width of the W boson: $\Gamma_W = 2.126 \pm 0.092$ GeV. CDF reports on a direct measurement of $\Gamma_W = 2.19 \pm 0.19$ GeV, in good agreement with the indirect determination and Standard Model predictions. DØ's measurement of the differential $d\sigma/dp_T$ distribution for W and Z bosons decaying to electrons agrees with the combined QCD perturbative and resummation calculations. In addition, the $d\sigma/dp_T$ distribution for the Z boson discriminates between different vector boson production models. Studies of $W + \text{Jet}$ production at CDF find the NLO QCD prediction for the production rate of $W + \geq 1$ Jet events to be in good agreement with the data.

1 Introduction

W and Z bosons, the carriers of the weak force, are directly produced in high energy $\bar{p}p$ collisions at the Fermilab Tevatron, which operates at a center of mass energy of $\sqrt{s} = 1.8$ TeV. In addition to probing electroweak physics, the study of the production of W and Z bosons provides an avenue to explore QCD, the theory of strong interactions. The benefits of using intermediate vector bosons to study perturbative QCD are large momentum transfer, distinctive event signatures, low backgrounds, and a well understood electroweak vertex.

Large numbers of W bosons have been detected by the two collider detectors (CDF and DØ), during the 1992–1996 running period. These samples complement the detailed studies carried out on the Z boson at LEP and SLC, and also the new W studies from LEP II. The CDF and DØ collaborations have used these data to perform various tests of the Standard Model. The preliminary results are presented in the next sections.

2 W and Z Production Cross Sections at $D\bar{O}$

The W and Z production cross sections times leptonic branching fractions are measured using data collected by the $D\bar{O}$ detector during 1994–1995, in the electron, muon and tau channels. The W candidates decaying to electrons or muons were selected as events containing one high quality isolated lepton and an imbalance of the momentum in the transverse plane of at least 25 GeV for electrons and 20 GeV for muons, as a signal for the undetected neutrino. The Z candidates decaying to electrons or muons were selected as events containing two high quality isolated leptons.

The major source of background in all four cases is due to QCD events with jets faking leptons. The amount of background in the samples is estimated directly from collider data. Backgrounds originating from other physics processes ($W \rightarrow \tau\nu_\tau$, $Z \rightarrow \tau\tau$, Drell–Yan) are estimated from Monte Carlo. Lepton selection efficiencies are determined from the $Z \rightarrow ll$ data. The geometric and kinematic acceptance is calculated from a fast Monte Carlo simulation of the $D\bar{O}$ detector. Table 1 shows the preliminary values for the cross sections measured from these samples.

Table 1: The $D\bar{O}$ preliminary cross sections for W and Z bosons.

	$W \rightarrow e\nu$	$Z \rightarrow ee$	$W \rightarrow \mu\nu_\mu$	$Z \rightarrow \mu\mu$
N_{obs}	59579	5705	10335	331
Background(%)	8.1 ± 0.9	4.8 ± 0.5	19.8 ± 1.9	11.6 ± 2.3
Efficiency(%)	70.0 ± 1.2	75.9 ± 1.2	26.0 ± 1.6	51.9 ± 3.6
Acceptance(%)	43.4 ± 1.5	34.2 ± 0.5	20.5 ± 0.2	4.9 ± 0.2
Luminosity [pb^{-1}]	75.9 ± 6.4	89.1 ± 7.5	65.3 ± 3.5	65.3 ± 3.5
$\sigma \cdot B$ [nb] ($\pm\text{stat}$)	2.38 ± 0.01	0.235 ± 0.003	2.38 ± 0.03	0.176 ± 0.011
($\pm\text{syst}$) ($\pm\text{lum}$)	$\pm 0.09 \pm 0.20$	$\pm 0.005 \pm 0.020$	$\pm 0.17 \pm 0.13$	$\pm 0.020 \pm 0.009$

Many common sources of systematic error cancel when taking the ratio of the W to Z production cross section times branching ratio, defined as

$$R \equiv \frac{\sigma(\bar{p}p \rightarrow W + X)B(W \rightarrow l\nu_l)}{\sigma(\bar{p}p \rightarrow Z + X)B(Z \rightarrow ll)}.$$

This ratio is of interest since it can be expressed as the product of calculable or well measured quantities:

$$R = \frac{\sigma_W}{\sigma_Z} \frac{\Gamma(W \rightarrow l\nu)}{\Gamma(Z \rightarrow l^+l^-)} \frac{\Gamma_Z}{\Gamma_W}.$$

For the combined electron and muon channels, $D\bar{O}$ measures

$$R = 10.48 \pm 0.43.$$

Using the LEP measurement¹ of $B(Z \rightarrow ll) = (3.367 \pm 0.006)\%$, and the theoretical calculation² of $\sigma_W/\sigma_Z = 3.33 \pm 0.03$, one obtains

$$B(W \rightarrow l\nu_l) = (10.59 \pm 0.44)\%.$$

Combining this result with a theoretical calculation of the W leptonic partial width³ $\Gamma(W \rightarrow l\nu_l) = 225.2 \pm 1.5$ MeV, results in a total width for the W boson of

$$\Gamma(W) = 2.126 \pm 0.092 \text{ GeV}.$$

This method, though model dependent, gives the most precise indirect measurement of the width of the W boson (Γ_W) currently available. All these results are in good agreement with previous $D\bar{O}$ results⁴, and with Standard Model predictions³.

DØ has also observed the production of $W \rightarrow \tau\nu_\tau$ and used it to test lepton universality. The τ lepton is identified via its hadronic decay, which is detected as an isolated, narrow jet, with $E_T(\text{jet}) > 25$ GeV and completely contained within DØ's central calorimeter. In addition, to select τ 's originating from W decays, a minimum imbalance in the transverse energy of 25 GeV is required. The Profile, defined as the sum of the two highest E_T towers divided by the transverse energy of the cluster, provides powerful discrimination against QCD multijet backgrounds. Jets originating from hadronic τ decays tend to be narrower than those originating in multijet QCD events, and therefore will show a higher value for the Profile distribution. The low-Profile region is used to estimate the QCD contamination in the final $W \rightarrow \tau\nu_\tau$ sample.

Events where more than one inelastic collision took place during the same beam crossing were rejected at the trigger level; this effectively reduced the integrated luminosity to ≈ 17 pb $^{-1}$ for the complete 1994–1995 DØ data sample. 1202 events pass these selection criteria, with estimated backgrounds of $106 \pm 7 \pm 5$ events from QCD, 81 ± 14 events from noisy calorimeter cells, 32 ± 5 events from $Z \rightarrow \tau\tau$, and 3 ± 1 events from $W \rightarrow e\nu$. The acceptance \times efficiency for the selection is $\approx 3.8\%$. The preliminary cross section times branching ratio obtained from this data is

$$\begin{aligned} \sigma(\bar{p}p \rightarrow W + X)B(W \rightarrow \tau\nu_\tau) &= 2.38 \\ &\pm 0.09 \text{ (stat)} \pm 0.10 \text{ (syst)} \pm 0.20 \text{ (lum)nb.} \end{aligned}$$

Comparing this measurement with DØ's published⁴ value for $\sigma \cdot B(W \rightarrow e\nu)$, measures the ratio of the couplings

$$g_\tau^W/g_e^W = 1.004 \pm 0.019 \pm 0.026.$$

This result shows good agreement with the expected $e - \tau$ universality.

3 Direct Measurement of the Width of the W at CDF

The indirect measurement of Γ_W presented in the previous section assumes that the W coupling to leptons is given by the Standard Model. Although in principle nonstandard couplings would also alter the W production cross section and thus affect the value of $\Gamma(W \rightarrow l\nu)/\Gamma_W$ extracted from R , a direct measurement of the total width of the W is desirable so that these radiative corrections to Γ_W can be observed.

It has been shown⁵ that the tail of the transverse mass M_T distribution of the W contains information on Γ_W . Events with $M_T > M_W$ can arise due to the nonzero W width or due to the calorimeter resolution. However, a precise measurement of Γ_W from the high mass tail is possible because far above M_W the Breit–Wigner tail dominates over the Gaussian resolution of the detector. In this analysis CDF uses data taken during the 1994–1996 Tevatron run to determine the W width from a binned log-likelihood fit to the transverse mass distribution in the region $110 < M_T(\text{GeV}/c^2) < 200$.

Monte Carlo templates are generated for different values of Γ_W and correspond to the sum of the W Monte Carlo and the backgrounds. The data are fitted to each template, and a likelihood curve vs Γ_W is made. The resulting likelihood is shown in the inset to figure 1. The most likely value for the total width of the W boson is $\Gamma_W = 2.19_{-0.16}^{+0.17}(\text{stat}) \pm 0.09(\text{syst})$ GeV. This result is in good agreement with the indirect measurement and the Standard Model prediction³.

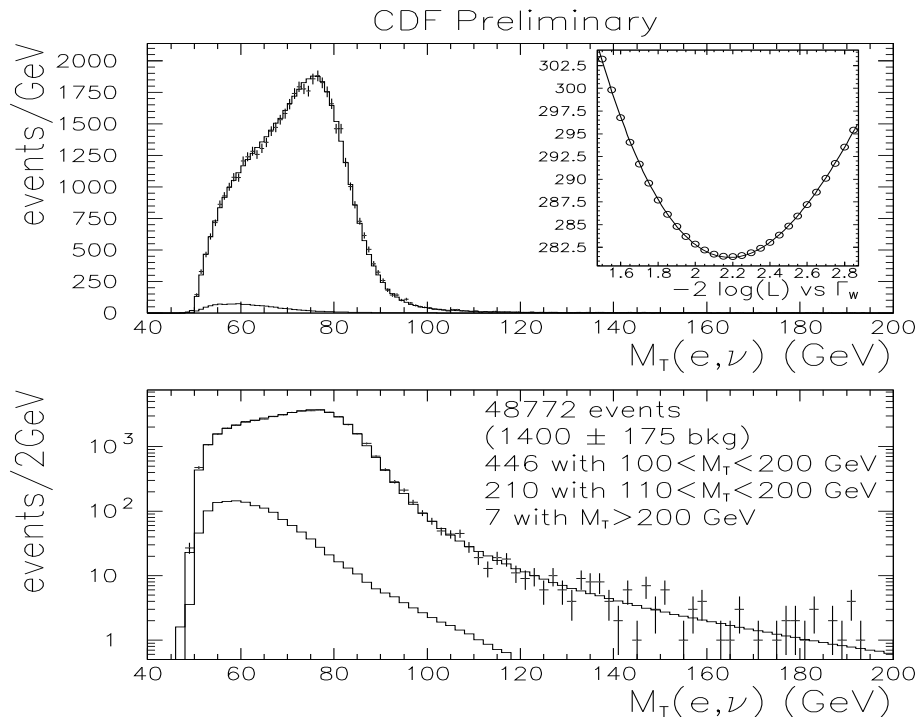


Figure 1: CDF W data transverse mass, with best fit overlaid. The size and shape of the summed backgrounds are also shown. Inset: Log-likelihood fit of the data to Monte Carlo templates of different W widths.

4 Measurement of the differential $d\sigma/dp_T$ Cross Sections at $D\bar{O}$

$D\bar{O}$ also measures the differential cross section for the W and the Z boson decaying to electrons, as a function of the boson transverse momentum. The transverse momentum (p_T) of intermediate vector bosons produced in proton-antiproton collisions is due to the production of one or more gluons or quarks along with the boson. At low transverse momentum ($p_T < 10$ GeV/ c), multiple soft gluon emission is expected to dominate the cross section. A soft gluon resummation technique^{6,7,8,9,10} is therefore used to make QCD predictions. At high transverse momentum ($p_T > 20$ GeV/ c), the cross section is dominated by the radiation of a single parton with large transverse momentum. Perturbative QCD¹¹ is therefore expected to be reliable in this regime. A prescription¹⁰ has been proposed for matching the low and high p_T regions to provide a continuous prediction for all p_T . Thus, a measurement of the transverse momentum distribution may be used to check the soft gluon resummation calculations in the low p_T range, and to test the perturbative QCD calculations at high p_T .

For this analysis, $D\bar{O}$ uses 7132 $W \rightarrow e\nu$ events collected during the 1992–1993 collider run, and 6407 $Z \rightarrow ee$ events from the 1994–1996 data set. The major source of background for both samples is QCD multi-jet and photon-jet events: the amount of background in the samples and its shape as a function of p_T is obtained directly from $D\bar{O}$ data. The variation of the trigger and selection efficiency vs p_T is calculated using a full detector Monte Carlo simulation. A parametrized representation of the $D\bar{O}$ detector is used to smear the theoretical prediction by detector effects and compare it to the measured p_T . The results are shown in figures 2 and 3 for the W and Z respectively. The W data shows good agreement with the combined QCD perturbative and resummation calculation. The Z data shows generally good agreement over the entire range, except for an approximately 2σ deviation near p_T^Z of 40 GeV/ c . In addition, figure 3 shows how the p_T^Z distribution departs from the pure perturbative QCD prediction at very low transverse momenta, which corroborates the known need for resummation in this

region.

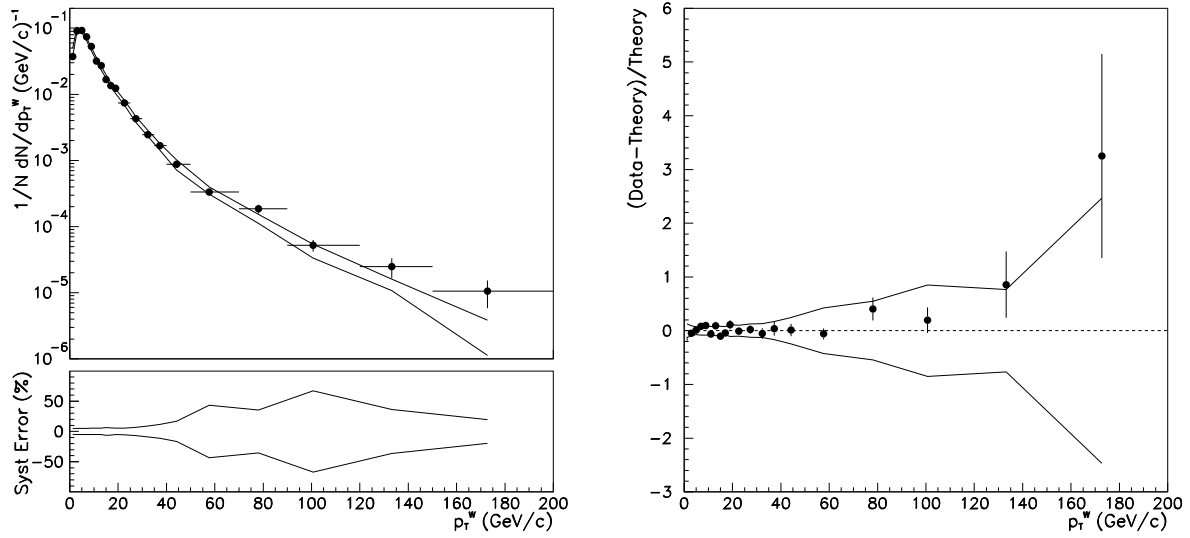


Figure 2: Left: $D\bar{O}$ data (solid points) with statistical uncertainty are compared to the theoretical prediction by Arnold-Kauffman[10], smeared for detector resolutions. Data and theory are independently area-normalized to unity. The fractional systematic uncertainty on the data is shown as a band in the lower portion of the plot. Right: The ratio $(\text{Data}-\text{Theory})/\text{Theory}$ shown as a function of p_T^W with its statistical uncertainty as error bars.

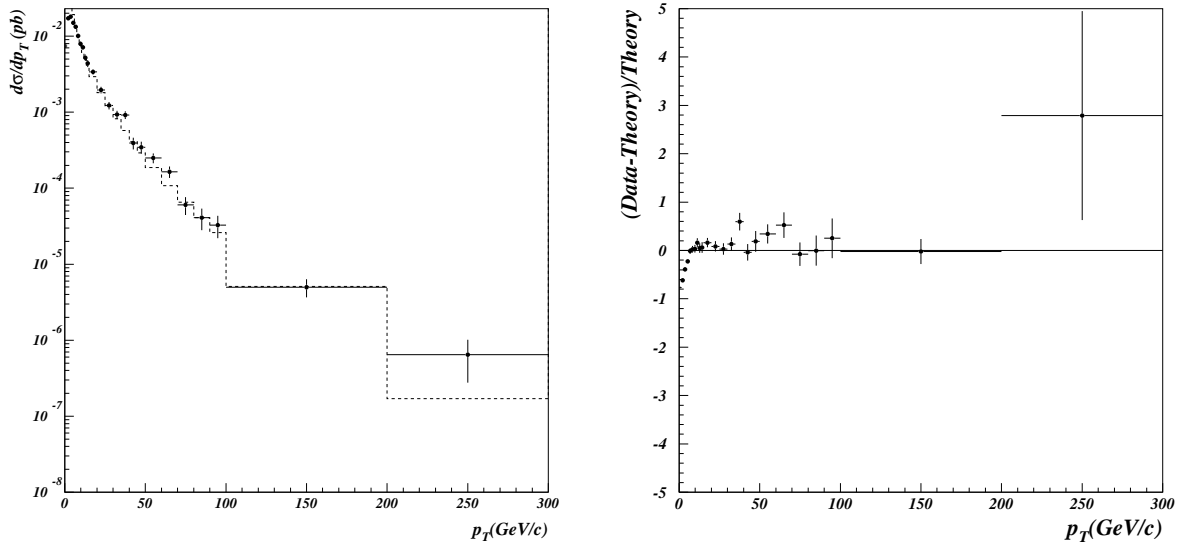


Figure 3: Left: $D\bar{0}$ data (solid points) with total uncertainty are compared to the theoretical prediction by Arnold-Reno[11], smeared for detector resolutions. Data is normalized to the measured inclusive Z production cross section presented in section 2; the theory is normalized to its own prediction. Right: The ratio $(\text{Data}-\text{Theory})/\text{Theory}$ as a function of p_T^Z clearly shows the known need for resummation in the very low p_T region.

Figure 4 shows that the p_T^Z distribution is able to distinguish between two available models^{9,10} for the non-perturbative contributions to the transverse momentum.

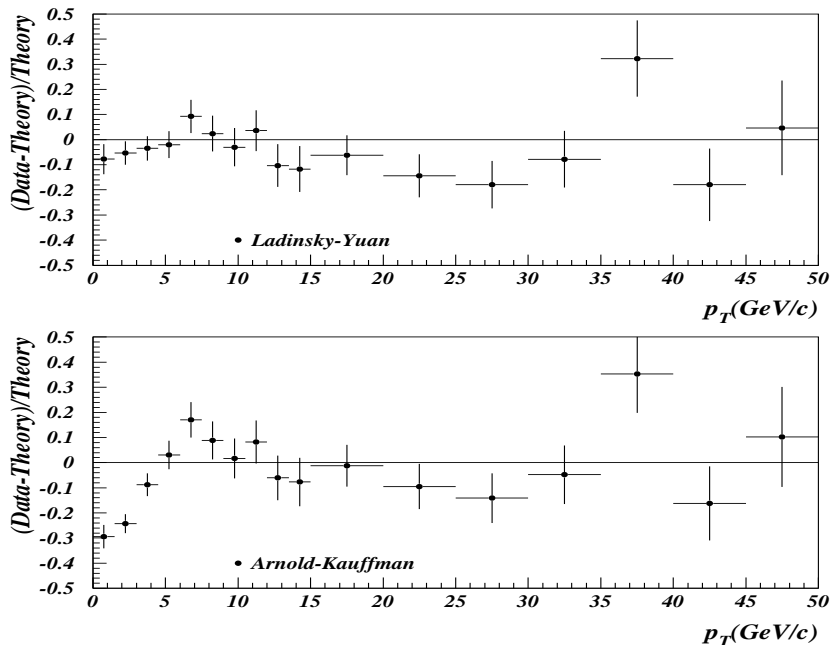


Figure 4: The ratio (Data-Theory)/Theory shown as a function of p_T^Z for two available models for the non-perturbative contribution: Ladinsky-Yuan [9] (top), and Arnold-Kauffman [10] (bottom).

5 Studies of $W + \text{Jets}$ Production at CDF

The CDF Collaboration uses 108 pb^{-1} of data, accumulated from 1992 to 1995, to measure the production cross section of $\sigma_n \equiv W + \geq n \text{ Jets}$ (for $n = 1, 4$) relative to the published ($W + \geq 0 \text{ Jets}$) inclusive cross section measurement for the 1992–1993 collider run¹². The analysis is restricted to events where the W decays into a central pseudorapidity electron ($|\eta_e| < 1.1$). The jets are reconstructed using a 0.4 fixed cone algorithm and restricted to $|\eta_{\text{Jet}}| < 2.4$.

The backgrounds to this sample are determined as a function of jet multiplicity in the event. The dominant background is due to QCD multijet events, and varies from $\approx 2.9\%$ to $\approx 27\%$ for the $n = 0$ to $n = 4$ case. The background originating from top quark and diboson production processes varies from $\approx 0.1\%$ to $\approx 17\%$ for the $n = 0$ to $n = 4$ case. Backgrounds from electroweak processes ($W \rightarrow \tau\nu_\tau$, $Z \rightarrow \tau\tau$ and $Z \rightarrow ee$) are estimated as a flat 3% contribution. The overall detection efficiency is $\approx 20\%$.

The measurement¹³ of σ_n is compared to predictions obtained from the leading order QCD matrix element calculations¹⁴ by including gluon radiation and hadronic fragmentation using the HERWIG¹⁵ shower simulation algorithm. The W boson events with hadron showers are then introduced into a full CDF detector simulation, and the resulting jets are identified and selected as in the data, allowing a comparison between the QCD predictions and the data.

Figure 5 shows the CDF data compared to the theoretical prediction for two choices of the renormalization and factorization scale $Q_{REN,FAC}^2$. The published $Z + \geq n \text{ Jets}$ cross section¹⁶ is also shown. One observes that the measured $W + \geq n \text{ Jets}$ cross sections are a factor of 1.7 larger than the LO QCD prediction for $Q_{REN,FAC}^2 = M^2(W) + p_T^2(W)$.

CDF uses the same data sample to measure $R_{10} \equiv \sigma(W + \geq 1 \text{ Jet})/\sigma(W)$, as a function of

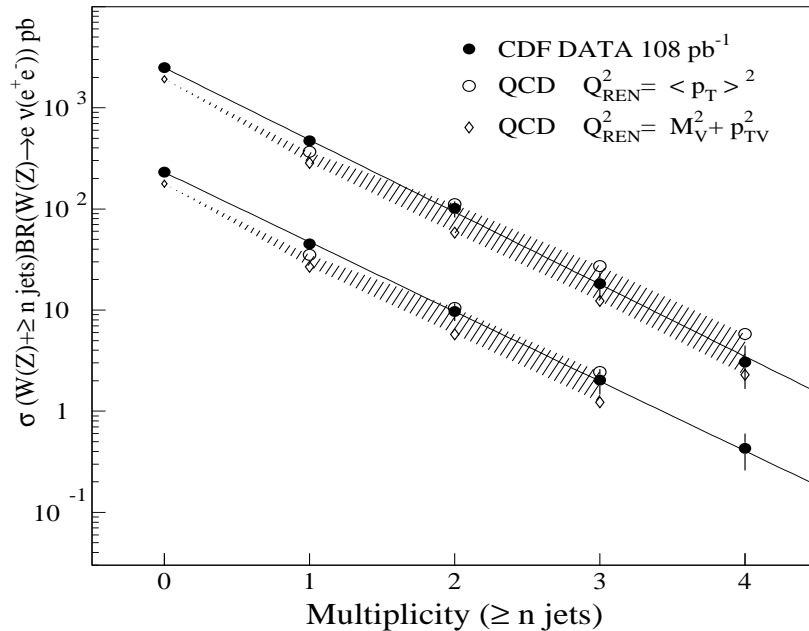


Figure 5: CDF's $\sigma_n(W + n \text{ Jets})$ as a function of the jet multiplicity. The result[12] for $\sigma_n(Z + n \text{ Jets})$ is also shown.

jet E_T threshold (E_T^{min}) in the 15 to 95 GeV range. The backgrounds to the $W + \geq 1$ Jet sample are determined as a function of E_T^{min} . The dominant background is due to QCD multijet events and varies from $\approx 13\%$ to $\approx 28\%$ for E_T^{min} of 15 to 95 GeV. The corresponding backgrounds originating from other physics processes vary from $\approx 5\%$ to $\approx 13\%$. The combined selection efficiency and acceptance varies from $\approx 19\%$ to $\approx 26\%$ as a function of jet E_T^{min} . For the inclusive W sample the total background level is $\approx 6\%$, and the combined selection efficiency and acceptance is $\approx 20\%$.

The measurement of R_{10} is compared to NLO QCD predictions obtained by the DYRAD Monte Carlo¹⁷. Figure 6 shows the measured R_{10} distribution as a function of E_T^{min} , compared to the theoretical prediction. The agreement over the full Jet E_T^{min} range is excellent, except for the lowest thresholds ($E_T^{min} < 25$ GeV), which is interpreted as an indication of the need of resummation in the calculation of the cross sections. Little variation is observed in the prediction when varying parton distribution functions (PDFs) or the normalization and factorization scales.

6 Conclusions

Using approximately 100 pb^{-1} of data each from Run 1 at the Tevatron, the CDF and DØ collaborations make precise measurements of the vector boson production properties that test QCD predictions. The measurements of the inclusive W and Z production cross sections agree with Standard Model predictions. The direct and indirect determinations of the total width of the W boson agree with each other and with expectations. The measured W and Z transverse momentum distributions agree with the combined QCD perturbative and resummation calculations; the Z boson data distinguish between different vector boson production models. CDF's measured $W + \geq n$ Jets cross sections are a factor of 1.7 larger than the LO QCD prediction for $Q_{REN,FAC}^2 = M^2(W) + p_T^2(W)$; the ratio of the production cross section of $W + \geq 1$ Jet events to the inclusive W sample (R_{10}) agrees with the NLO QCD prediction.

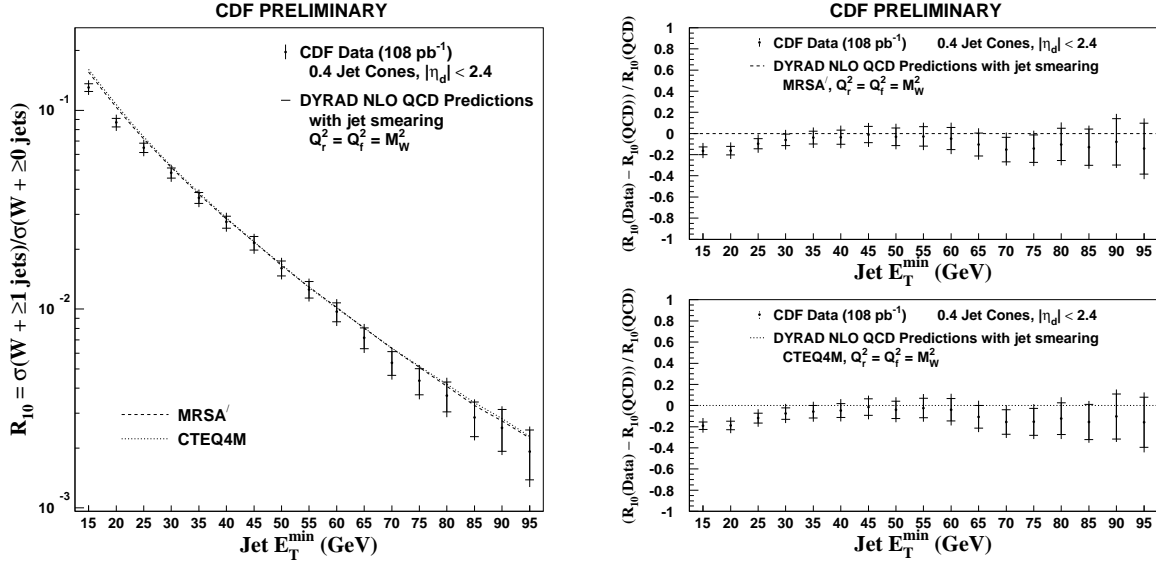


Figure 6: CDF's measurement of $R_{10} \equiv \sigma(W + \geq 1 \text{ Jet}) / \sigma(W)$, as a function of jet E_T^{\min} , compared to NLO QCD prediction by [17]. The (Data–Theory)/Theory plot is shown at the right for two choices of PDFs.

Acknowledgments

We acknowledge the support of the US Department of Energy and the $D\bar{0}$ and CDF collaborating institutions and their funding agencies in this work.

References

1. Particle Data Group, L. Montanet *et al.*, Phys. Rev. **D50**, 1173 (1994.)
2. H. Hamberg *et al.*, Nucl. Phys. **B359**, 343 (1991);
W.L. van Neerven and E.B. Zijlstra, Nucl. Phys. **B382**, 11 (1992.)
3. J.L. Rosner, M.P. Worah, and T. Takeushi, Phys. Rev. **D49**, 1363 (1994.)
4. S. Abachi *et al.*, *Phys. Rev. Lett.* **75** 145695.
5. F. Abe *et al.*, Phys. Rev. Lett. **74** 34195.
6. J. Collins, D. Soper, and G. Sterman, Nucl. Phys. **B250**, 199 (1985); J. Collins and D. Soper, Nucl. Phys. **B193**, 381 (1981), Nucl. Phys. **B197**, 446 (1982), and erratum Nucl. Phys. **B213**, 545 (1983).
7. C. Davies, B. Webber, and W. J. Stirling, Nucl. Phys. **B256**, 413 (1985); C. Davies and W. J. Stirling, Nucl. Phys. **B244**, 337 (1984).
8. G. Altarelli, R. K. Ellis, M. Greco, and G. Martinelli, Nucl. Phys. **B246**, 12 (1984).
9. G. A. Ladinsky and C. P. Yuan, Phys. Rev. **D50**, 4239 (1994.)
10. P. Arnold and R. Kauffman, Nucl. Phys. **B349**, 381 (1991.)
11. P. B. Arnold and M. H. Reno, Nucl. Phys. **B319**, 37 (1989); R. J. Gonsalves, J. Pawlowski, and C-F. Wai, Phys. Rev. D **40**, 2245 (1989).
12. F. Abe *et al.*, *Phys. Rev. Lett.* **76** 307096.
13. F. Abe *et al.*, Phys. Rev. Lett. **79** 476097.
14. F. A. Berends *et al.*, Nucl. Phys. **B357**, 32 (1991.)
15. G. Marchesini and B. Webber, Nucl. Phys. **B310**, 461 (1988.)
16. F. Abe *et al.*, *Phys. Rev. Lett.* **77** 44896.
17. W. T. Giele *et al.*, Nucl. Phys. **B403**, 633 (1993.)